J. King Saud Univ., Vol. 3, *Eng. Sci.* (2), pp. 167–183 (1411 A.H./1991)

Deformational Behavior of Reinforced Concrete Beams under Service Loading Conditions

Rajeh Z. Al-Zaid, M.M. Abu-Hussein* and A.H. Al-Shaikh
*Assistant Professors and *Graduate Student, Civil Engineering Department, College of Engineering, King Saud University, P.O. Box 800, Riyadh 11421, Saudi Arabia*

Abstract. The paper presents the results of an experimental study conducted on model-size reinforced concrete beams aiming at quantifying the effect of cracking under various types of loading on their deflection responses. A central, third-points, uniformly distributed, and a combination of a central and uniformly distributed loads are considered. The test results indicate that, at the same level of maximum moment, the effective moment of inertia is significantly affected by the type of loading. A general model is proposed for estimating the effective moment of inertia of reinforced concrete beams under any arbitrary symmetrical loading. The accuracy of the model is checked by comparing with test results available in literature.

Notation

The following symbols are used in this paper:

C = depth to neutral axia of the reinforced concrete section;

E_c = modulus of elasticity of concrete;

f'_c = compressive strength of concrete;

f_r = modulus of rupture of concrete;

h = total depth of concrete section;

I_{cr} = moment of inertia of the cracked transformed reinforced concrete section;

I_e = effective moment of inertia of the cracked reinforced concrete beam;

I_g = moment of inertia of the gross concrete section;

L = length of beam span;

L_{cr} = theoretical cracked length of the beam;

M_a = maximum service load moment acting on the beam;

M_{cr} = cracking moment of beam $= f_r . \frac{I_g}{h - C}$

P = total machine load;

P_{cr} = cracking load;

ε_s = strain in tension reinforcement;

ε'_s = strain in compression reinforcement;

Δ = maximum deflection;

ρ = reinforcement ratio;

ρ_b = reinforcement ratio producing a balanced condition;

ϕ = curvature at midspan section.

Introduction

New advancements in structural materials and design procedures have resulted in more slender, hence more deformable, structural members. Due to the complex nature of the deflection response of reinforced concrete beams and the desirability of having a simplified method for calculating instantaneous deflections, various procedures have been proposed [1-4].

In 1963 Branson [5] presented an empirical expression for the effective moment of inertia (I_e) assumed the same over the entire length of a cracked simply supported beam; it is of the form:

$$I_e = (M_{cr}/M_a)^3 I_g + \{ 1 - (M_{cr}/M_a)^3 \} I_{cr} \leq I_g \quad (1)$$

The only load parameter in Eq. (1) is the maximum moment (M_a) at which I_e is estimated. Hence, Eq. (1) will lead to the same I_e for all identical beams loaded to the same level of maximum moment (M_a) irrespective of the type of the applied load.

Fig. 1 shows a typical curve of the cracked length ratio (L_{cr}/L) v.s. the level of loading indicated by the ratio Ma_a/M_{cr} under various types of loading. The cracked length is defined as the beam segment over which the working moment exceeds the cracking moment (M_{cr}). The figure shows that, for the same value of maximum moment (M_a), centrally loaded beams will have less cracked lengths than uniformly loaded beams and beams loaded at third points. This phenomenon is expected to

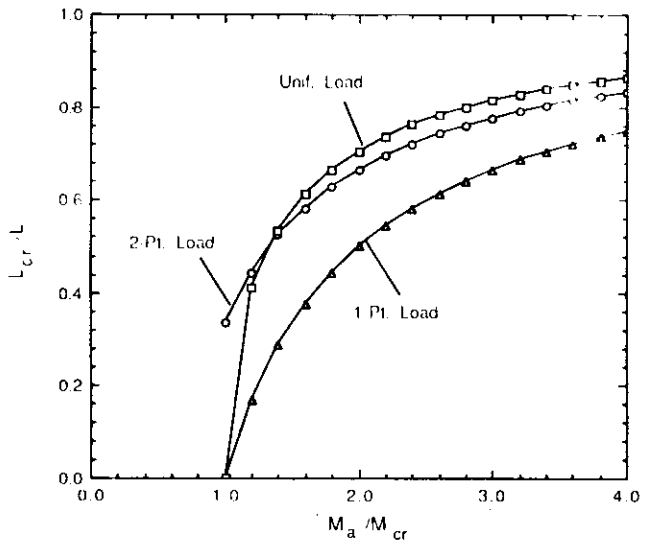

Fig. 1. Theoretical variation of cracked length ratio with the level of maximum moment for different types of loading.

result in different values of effective moments of inertia for differently loaded identical beams under the same level of M_a/M_{cr} ratio. Such a difference is not recognized by Eq. (1). It should be noted that the theoretical cracked length (L_{cr}) can be easily determined using the fundamentals of structural analysis.

Objective of the Study

The objective of this study is to quantify experimentally the effect of type of loading on the effective moment of inertia of cracked reinforced concrete beams. The experimental results are then used to develop an empirical model for estimating the effective moment of inertia which takes into account the effect of type of loading.

Test Specimens and Material Properties

All test beams were of rectangular cross sections with dimensions 200×200×2900 mm and reinforcement ratio of 0.4 ρ_b. The beams were tested over a simple span of 2500 mm. To avoid shear failures, all beams were provided with ϕ6 mm stirrups at 70 mm center to center spacing. One ϕ10 mm bar was used as an anchor bar at the top of each beam. The beams were cured under damp burlap for 27 days and tested one day later. Details of test beams are shown in Fig. 2. In the beam designation, the letters U,C,T, and CU stand for beams tested under

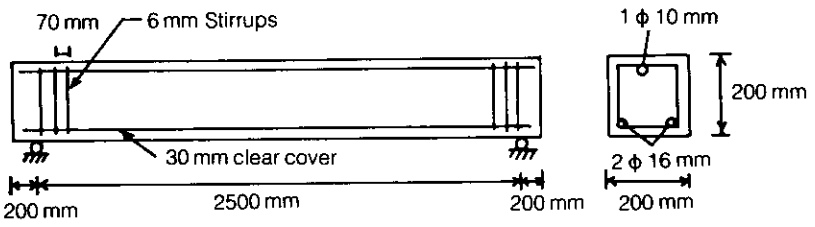

Fig. 2. Details of test beams

uniformly distributed, centrally, third-points and combined centrally and uniformly distributed loads, respectively.

Ready-mixed concrete with maximum size of aggregate of 10 mm was used throughout and had a slump of 80 mm. The mix proportions were 1: 1.8: 3.4 by weight with a water-cement ratio of 0.56 and a design characteristic strength of 34 MPa (5 ksi). Three concrete batches were cast with average compressive strengths of 38.2, 38.2 and 31.4 MPa. The compressive strength of concrete (f'_c) was determined by testing 152 mm diameter by 305 mm high (6 in × 12 in.) concrete cylinders. Five cylinders were cast from each batch and cured under similar conditions to those of the beams and were tested one day before testing the beams. Grade 60 deformed steel bars were used and the modulus of elasticity of steel (E_s) was taken as 2×10^5 MPa (29000 ksi).

Loading System and Instrumentation

A set of four identical pairs of simply supported beams were tested for load deflection response under a central, third-points, uniformly distributed, and a combination of a central and uniformly distributed loading. The combined load is considered here as a typical example for actually loaded beams where a central load might exist beside the uniform dead weight of the beam.

All beams were tested using the 200-Tons Amsler Universal testing machine shown in Fig. 3. One or two roller supports were attached to the upper platten to apply an adjustable one-point or two-point load. The uniformly distributed and the combined central and uniformly distributed loads were simulated using the arrangements shown in Fig. 4.

Two dial gauges with 0.01 mm accuracy were used to measure the maximum deflection at midspan of each beam. The average of the two dial gauge readings was taken as the beam deflection. In order to plot the M-ϕ curves for the test beams, strains in both tension and compression steels were recorded using electrical resistance strain gauges (ersg).

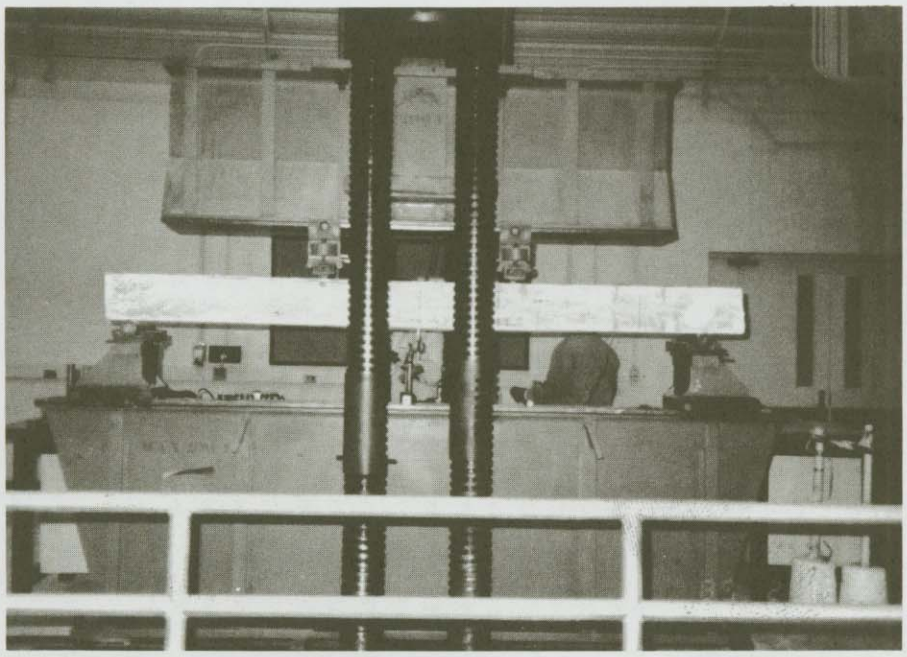

Fig. 3. Testing machine and test setup

Analysis and Discussion of Test Results

The test results as well as the computed parameters of concern are summarized in Tables 1, 2, 3, and 4. The deflection values are the average values of two identically loaded beams. A Typical load-deflection curve is shown in Fig. 5.

For each type of loading, the process of analyzing the results involved the following computations:

1) The cracking load is obtained from the average load-deflection curve of the two identically loaded beams at point of deviation from linearity.

2) The experimental effective moment of inertia (I_{exp}) for each pair of beams is determined from the measured deflections using the well known elastic deflection formula expressed in the following form:

$$I_{exp} = K \frac{M_a L^2}{E_c \triangle} \tag{2}$$

Table 1. Test results and analysis of beams B1-U and B2-U

Total load P(kN) (1)	M_a/M_{cr} (2)	Defl. Δ (mm) (3)	ε_s (10^{-6}) (4)	ε'_s (10^{-6}) (5)	I_{exp} ($mm^4 \times 10^4$) (6)	ϕ ($mm^{-1} \times 10^{-6}$) (7)	C (mm) (8)	L_{cr}/L (9)	m (10)	I_{exp}/I_e, Eq. (1) (11)	I_{exp}/I_e, Eq. (5) (12)
3.92	0.25	0.20	19.0	–16.0	–	0.307	93.1	0	–	–	–
7.84	0.49	0.38	34.8	–30.0	–	0.568	93.8	0	–	–	–
11.77	0.74	0.58	54.5	–44.0	–	0.864	91.9	0	–	–	–
15.69	1.00	0.95	267.5	–67.0	–	2.93	63.7	0	–	–	–
19.61	1.23	1.67	397.0	–76.0	8399	4.149	59.3	0.44	0.80	–	–
23.53	1.48	2.5	737.0	–72.0	6732	7.096	51.1	0.57	0.65	1.00	1.18
27.45	1.73	3.33	894.0	–67.0	5896	8.43	48.9	0.65	0.58	1.05	1.11
31.38	1.98	4.13	1035.0	–64.5	5434	9.65	47.7	0.70	0.53	1.08	1.07
35.30	2.22	5.01	1179.0	–61.0	5036	10.88	46.6	0.74	0.46	1.08	1.03
39.22	2.47	5.90	1328.0	–57.0	4754	12.15	45.7	0.77	0.40	1.07	1.00
43.14	2.72	6.73	1341.0	–58.0	4585	12.28	45.7	0.79	0.37	1.07	0.98
47.07	2.96	7.55	1610.0	–58.0	4458	14.63	45.0	0.81	0.34	1.07	0.98
50.99	3.21	8.36	1744.0	–56.5	4362	15.80	44.6	0.83	0.33	1.07	0.97
54.91	3.46	9.17	1864.0	–60.0	4283	16.88	44.1	0.84	0.30	1.06	0.96
58.83	3.70	10.07	1985.0	–56.0	4178	17.90	44.1	0.85	0.25	1.05	0.95

Note: f'_c = 38.2 MPa (5.5 ksi), E_c = 29634 MPa (4300 ksi),
$I_{cr} = 38.0 \times 10^6$ mm^4 (91.3 in^4), and M_{cr} = 5.2 kN.m (45.73 in.–kips)
as obtained from the load deflection curve.

Table 2. Test results and analysis of beams B3-C and B4-C

Total load P(kN) (1)	M_a/M_{cr} (2)	Defl. Δ (mm) (3)	ε_s (10^{-6}) (4)	ε'_s (10^{-6}) (5)	I_{exp} ($mm^4 \times 10^4$) (6)	ϕ ($mm^{-1} \times 10^{-6}$) (7)	C (mm) (8)	L_{cr}/L (9)	m (10)	I_{exp}/I_e, Eq. (1) (11)	I_{exp}/I_e, Eq. (5) (12)
3.92	0.46	0.29	33.0	–20.5	–	0.469	84.7	0.0	–	–	–
7.84	0.92	0.65	96.5	–49.0	–	1.28	79.4	0.0	–	–	–
11.77	1.38	1.5	573.0	–64.0	8617	5.59	52.5	0.28	0.55	1.16	1.13
15.69	1.84	2.5	817.5	–59.0	6894	7.69	48.7	0.46	0.51	1.29	1.09
19.61	2.30	3.68	1054.0	–52.0	5854	9.70	46.4	0.57	0.43	1.28	1.02
23.53	2.76	4.77	1268.0	–44.0	5420	11.51	44.8	0.64	0.42	1.27	1.01
27.45	3.22	6.03	–	–	5002	–	–	0.69	0.36	1.22	0.98
31.38	3.68	7.31	1703.0	–29.5	4715	15.20	43.0	0.73	0.32	1.18	0.96
35.30	4.14	8.47	1912.0	–24.0	4578	16.98	42.4	0.76	0.31	1.16	0.96
39.22	4.6	9.65	2120.0	–19.0	4465	18.76	42.0	0.78	0.29	1.15	0.95

Note: f'_c = 38.2 MPa (5.5 ksi), E_c = 29634 MPa (4300 ksi),
$I_{cr} = 38.0 \times 10^6$ mm^4 (91.3 in^4), and M_{cr} = 5.3 kN.m (47.2 in.–kips)
as obtained from the load deflection curve.

Table 3. Test results and analysis of beams B5-T and B6-T

Total load P(kN) (1)	M_a/M_{cr} (2)	Defl. Δ (mm) (3)	ε_s (10^{-6}) (4)	ε'_s (10^{-6}) (5)	I_{exp} ($mm^4 \times 10^4$) (6)	ϕ ($mm^{-1} \times 10^{-6}$) (7)	C (mm) (8)	L_{cr}/L (9)	m (10)	I_{exp}/I_e, Eq. (1) (11)	I_{exp}/I_e, Eq. (5) (12)
3.92	0.36	0.26	14.3	–20.0	–	0.301	107.5	0.0	–	–	–
7.84	0.73	0.48	31.8	–36.0	–	0.595	101.6	0.0	–	–	–
11.77	1.09	1.12	94.5	–60.0	9831	1.360	85.3	0.39	1.06	–	–
15.69	1.45	1.87	181.0	–71.0	7953	2.215	73.3	0.54	0.93	1.15	1.35
19.61	1.82	2.91	317.0	–76.0	6306	3.440	63.0	0.63	0.66	1.17	1.17
23.53	2.18	4.12	458.0	–80.0	5345	4.720	58.0	0.69	0.48	1.13	1.04
27.45	2.55	5.09	621.8	–77.0	5048	6.130	53.6	0.74	0.47	1.15	1.03
29.42	2.73	5.65	700.5	–79.0	4872	6.840	52.6	0.76	0.43	1.14	1.02
33.34	3.09	6.83	1167.5	–41.0	4568	10.60	44.9	0.78	0.34	1.11	0.97
37.26	3.45	7.78	1338.0	–26.5	4482	11.97	43.3	0.81	0.35	1.11	0.98
41.18	3.82	8.69	1493.0	–17.5	4435	13.25	42.3	0.83	0.37	1.12	0.99
45.11	4.18	9.92	1674.0	–11.0	4255	14.78	41.7	0.84	0.28	1.08	0.96
49.03	4.55	10.84	1827.0	– 8.0	4234	16.09	41.5	0.85	0.29	1.09	0.96
52.95	4.91	11.80	1994.0	– 6.0	4199	17.54	41.3	0.86	0.28	1.08	0.96
56.87	5.27	12.87	2141.0	– 6.0	4135	18.83	41.3	0.87	0.26	1.07	0.96

Note: f'_c = 38.2 MPa (5.5 ksi), E_c = 29634 MPa (4300 ksi),
$I_{cr} = 38.0 \times 10^6$ mm^4 (91.3 in^4), and M_{cr} = 4.5 kN.m (39.92 in.–kips)
as obtained from the load deflection curve.

Table 4. Comparison of test results of beams B-7-CU and B8-CU with Eq. (5)

Total load P(kN) (1)	P_c (kN) (2)	W (kN/m) (3)	M_a/M_{cr} (4)	Defl. Δ (mm) (5)	I_{exp} ($mm^4 \times 10^4$) (6)	L_{cr}/L (7)	I_e, Eq. (5) ($mm^4 \times 10^4$ (8)	I_{exp}/I_e Eq. (1) (9)	I_{exp}/I_e, Eq. (5) (10)
11.77	8.09	1.47	1.28	1.47	8650	0.244	8076	1.02	1.07
15.69	10.79	1.96	1.70	2.57	6597	0.453	6599	1.10	1.00
19.61	13.48	2.45	2.13	3.70	5728	0.571	5946	1.14	0.96
23.53	16.18	2.94	2.55	4.6	5529	0.647	5567	1.19	0.99
27.46	18.88	3.43	2.98	5.63	5270	0.70	5318	1.19	0.99
33.34	22.92	4.17	3.62	7.22	4990	0.755	5073	1.16	0.98
37.26	25.61	4.66	4.04	8.27	4869	0.782	4956	1.15	0.98
41.18	28.31	5.15	4.47	9.30	4785	0.803	4867	1.14	0.98
45.11	31.01	5.64	4.89	10.40	4687	0.821	4791	1.12	0.98
49.03	33.70	6.13	5.32	11.33	4676	0.836	4729	1.13	0.99

Note: f'_c = 31.4 MPa (4.5 ksi), E_c = 26840 MPa (3892 ksi),
$I_{cr} = 40.9 \times 10^6$ mm^4 (98.26 in^4), and M_{cr} = 4.9 kN.m (43.39 in.–kips)
as obtained from the load deflection curve.

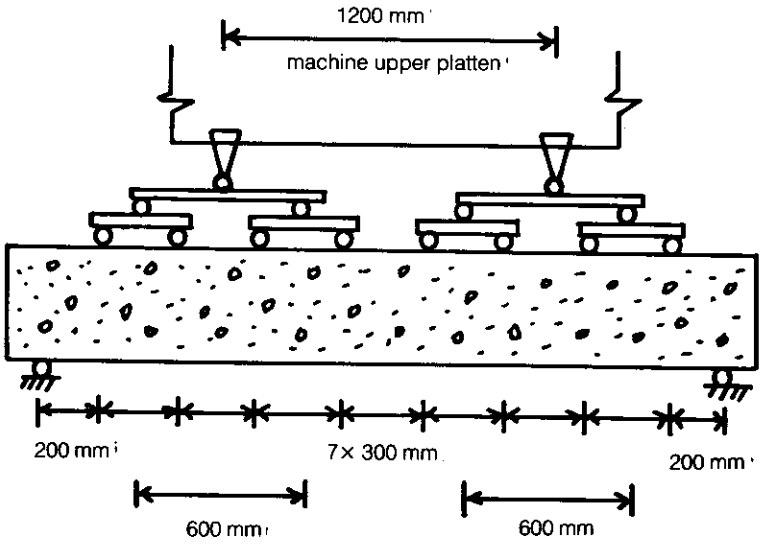

a) Uniform loading

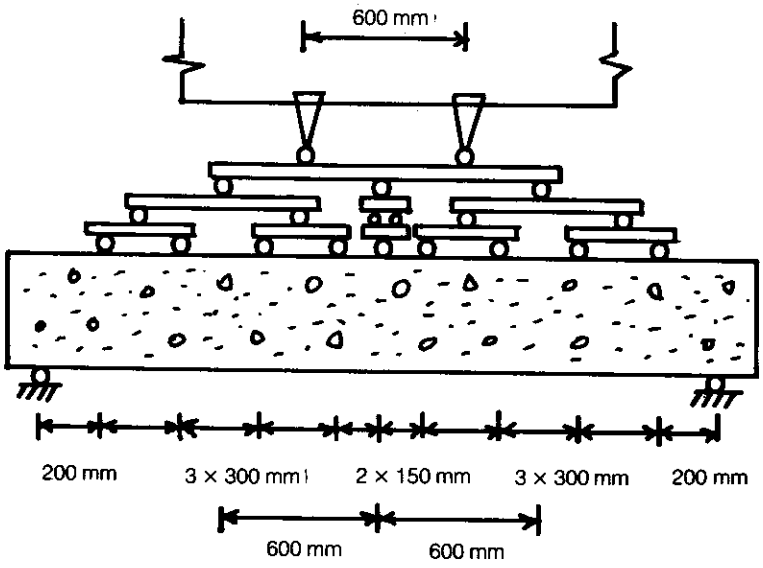

b) Combined central and uniformly distributed loading

Fig. 4. Arrangements used for uniformly distributed and combined loadings.

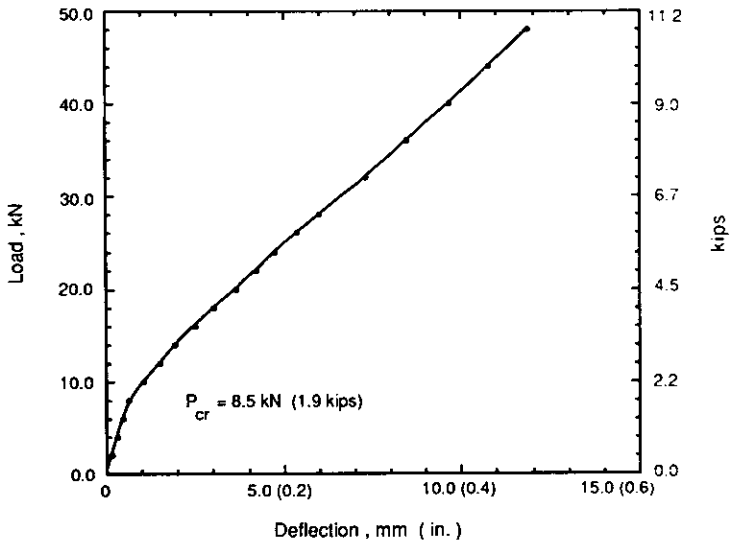

Fig. 5. Observed load-deflection behavior of beams B3 - C and B4 - C.

where K is a constant which depends on the type of loading and end conditions (*e.g* K = 5/48 and $M_a = \omega L^2/8$ for a uniformly loaded simple beam).

3) The depth of neutral axis (C) and curvature (ϕ) at midspan sections are determined using the measured strains in the tension and compression steel.

Moment-curvature relationships for the first three sets of test beams are shown in Fig. 6. The corresponding variations of the centroidal axis location with the moment level are shown in Fig. 7. The smooth transition between the uncracked and cracked states for third-points loading indicated in Fig. 7 is due to the fact that this case of loading is supposed to provide better crack distribution.

The variations of the experimental values of the effective moment of inertia (I_e) for the differently loaded beams with M_a/M_{cr} ratio are shown in Fig. 8. The figure reveals that differently loaded beams will have different values of the effective moment of inertia at the same M_a/M_{cr} level. This observation is physically explained by the difference in the cracked length indicated in Fig. 1.

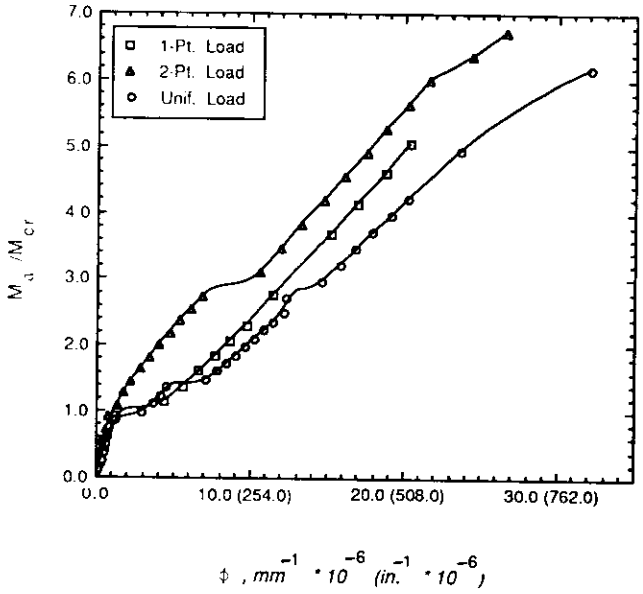

Fig. 6. Moment-curvature relationships of test beams

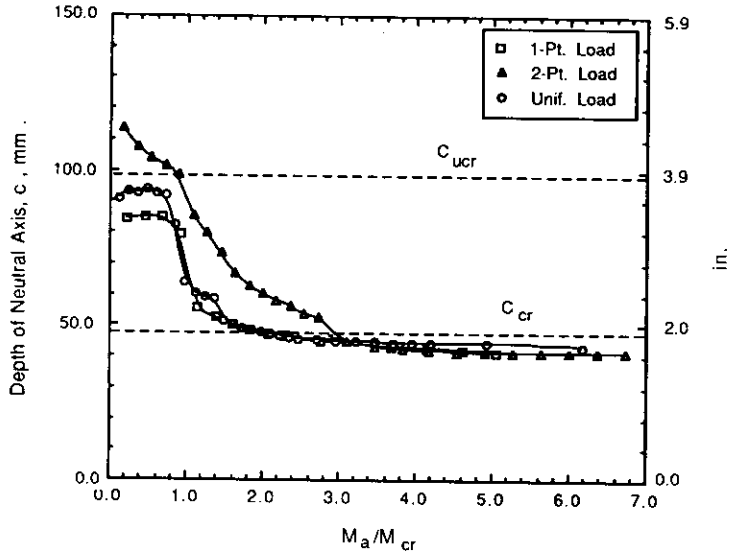

Fig. 7. Variation of depth of neutral axis with M_a / M_{cr} ratio

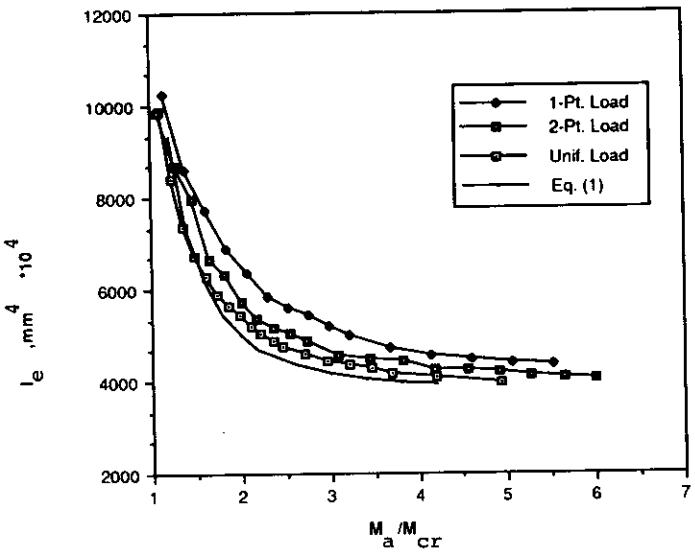

Fig. 8. Variation of I_e with M_a / M_{cr} ratio

Proposed Model

The experimental results depicted in Fig. 8 reveal that for the expression of the effective moment of inertia of a cracked reinforced concrete beam to be general, it has to incorporate a parameter which can measure both the severity of crack propagation and the extension of cracking along the beam. It is believed that the cracked length ratio (L_{cr}/L) may be such a parameter and therefore a model of the form given by the following equation is proposed:

$$I_e = (L_{cr}/L)^m I_{cr} + \{ 1 - (L_{cr}/L)^m \} I_g \tag{3}$$

The value of the exponent (m) is expected to be unique for all types of loading. It is to be determined experimentally using Eq. (4), which is obtained from Eq. (3).

$$m = \text{Log}\left(\frac{I_g - I_{exp}}{I_g - I_{cr}} \right) / \text{Log}\left(\frac{L_{cr}}{L} \right) \tag{4}$$

For symmetrically loaded simple beams, the exponent (m) is expected to be less than unity to magnify the effect of the cracking moment of inertia (I_{cr}) which dominates at the mid portion of the beam. Eq. (3) satisfies the limiting values of $I_e = I_g$ when $L_{cr} = 0$, while I_e approaches I_{cr} when L_{cr} approaches L.

The exponent (m) to be used in Eq. (3) was determined from the experimental results of the first three sets of test beams using Eq. (4) and is contained in column 10 of Tables 1 through 3. It varies from about 1.0 to 0.2 for all types of loading with a decreasing value as the cracked length (L_{cr}) increases. For practical considerations, an average value of 0.4 was found to give a fairly accurate prediction of I_e using Eq. (3) for the differently loaded beams particularly in the range of M_a/M_{cr} ratio greater than 1.5. Thus, the proposed model for the effective moment of inertia is given by

$$I_e = \left(\frac{L_{cr}}{L}\right)^{0.4} I_{cr} + \left\{1 - \left(\frac{L_{cr}}{L}\right)^{0.4}\right\} I_g \qquad (5)$$

Comparisons between the experimental and computed I_e values using both Eqs. (1) and (5) for the first three sets of test beams are presented in Tables 1 through 3. For instance, the results presented in Table 2 for beams tested under a mid-span concentrated load show a difference of up to 29% between the experimental and computed I_e values using Eq. (1) with an average value of about 22%. The corresponding average difference obtained using Eq. (5) is about 4%.

Eqs. (1) and (5) are also used to compute the I_e values for beams tested under combined loading and compared with the experimental results as shown in Table 4. The accuracy of Eq. (5) can easily be observed by referring to column 10 of Table 4.

The accuracy of the model can also be observed by referring to Fig. 9 where the computed and experimental values of I_e are plotted against the L_{cr}/L ratio for all types of loading.

Comparison with Previous Test Results

The applicability of the proposed model to the results of test beams available in literature was investigated. Six pairs of beams with rectangular sections [6] and six beams with T-sections [7] tested under uniformly distributed loads were considered for the comparison. The estimated experimental values of I_e of these beams and the beams tested in this study at randomly selected values of M_a/M_{cr} between 1.5 and 4.0 are plotted against the computed values of I_e using Eq. (5). The results are shown in Fig. 10. The figure shows that all the data points lie within the $\pm$ 15% limits which indicates that the model is reasonably accurate in predicting the I_e values for both rectangular and T-beams.

Conclusions

The following conclusions can be drawn from the test results of this study:

1) The effective moment of inertia of a cracked reinforced concrete beam is not only affected by the level of crack propagation but also by the extension of

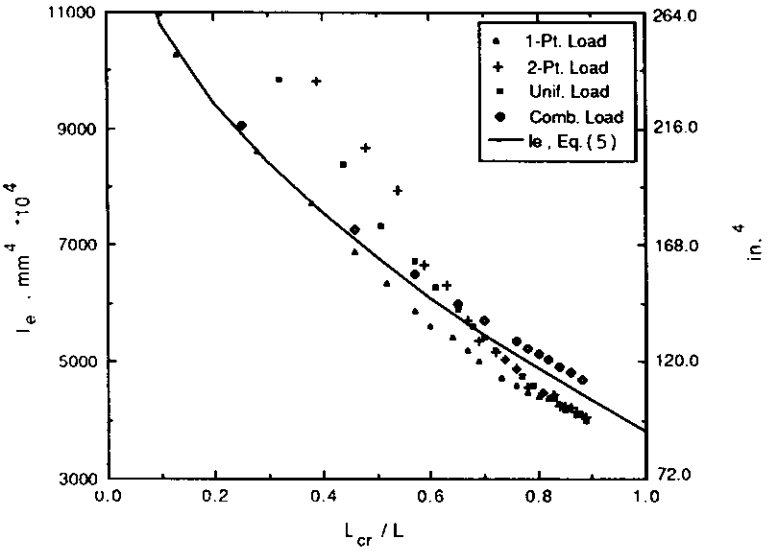

Fig. 9. Comparison of experimental I_e as function of L_{cr} / L ratio with Eq. (5)

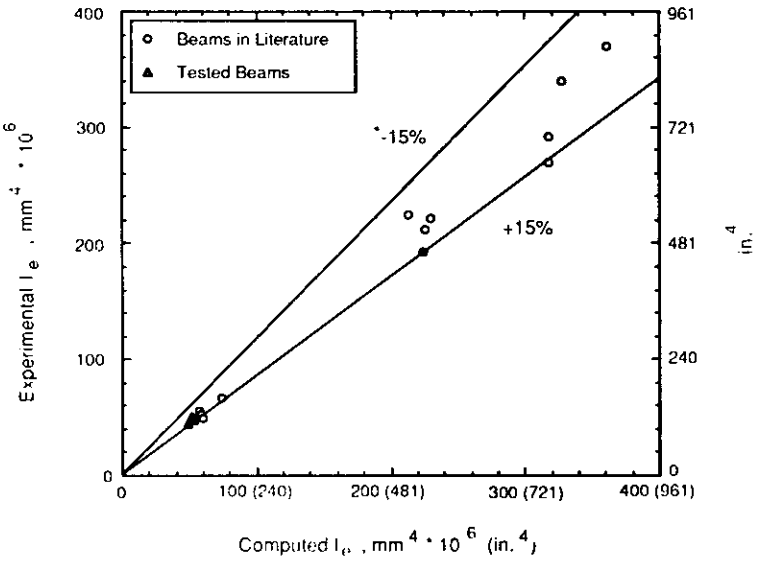

Fig. 10. Comparison of experimental I_e with computed I_e using Eq. (5)

cracking along the beam. Thus, differently loaded beams will have different effective moments of inertia under the same maximum moment. The observed ratio between I_e of a centrally loaded beam and that of a uniformly loaded beam is about 1.2.

2) For beams tested under a mid-span concentrated load, a difference of up to 29% between the experimental and computed I_e values using Eq. (1) was obtained with an average value of about 22%. The corresponding average difference using Eq. (5) was about 4%.

3) To account for the effects of load level and the extension of cracking along the beam under various types of loading, the model given by Eq. (5) is proposed for normally reinforced concrete beams.

4) Comparison of predicted test results with experimental results available in the literature indicates a very good accuracy of the proposed model.

References

[1] ACI Committee 435. "Deflections of Reinforced Concrete Flexural Members." *ACI Journal*, 63, No. 6 (1966), 637-674.

[2] Branson, D.E. *Deformation of Concrete Structures*. New York: McGraw-Hill Book Co., 1977.

[3] Abu-Hussein, M.M. "Effective Moment of Inertia of Cracked Reinforced Concrete beams Under Different Types of Loading." *M. Sc. Thesis*, King Saud University, June (1989), p. 116.

[4] ACI Committee 318. *Building Code Requirements for Reinforced Concrete* (ACI 318-87). Detroit: American Concrete Institute, 1987.

[5] Branson, D.E. "Instantaneous and Time-Dependent Deflections of Simple and Continuous Reinforced Concrete Beams." *HPR Report* No. 7, Part 1, Alabama Highway Department, Bureau of Public Roads, Aug. (1963), 78.

[6] Washa, G.W. and Fluck, P.G. "Effect of Compressive Reinforcement on the Plastic Flow of Reinforced Concrete Beams." *ACI Journal*, 49, No. 8 (1952), 89-108.

[7] Yu. W. and Winter, G. "Instantaneous and Long-Time Deflections of Reinforced Concrete Beams under Working Loads." *ACI Journal*, 57, No. 1 (1960), 29-50.

انحراف العوارض الخرسانية المسلحة تحت تأثير أحمال التشغيل

راجح زيد الزيد، مصطفى منير أبوحسين*، عبدالرحمن حسن آل الشيخ
قسم الهندسة المدنية، كلية الهندسة، جامعة الملك سعود، ص.ب ٨٠٠
الرياض ١١٤٢١، المملكة العربية السعودية

ملخص البحث. يعرض هذا البحث نتائج دراسة تجريبية عملت على نماذج مصغرة لعوارض خرسانية مسلحة لغرض تقويم أثر التشقق تحت تأثير أحمال مختلفة على أدائها الانحرافي، مثل الحمل المركز في نقطة عند منتصف العارضة أو نقطتين عند ثلثي العارضة، الحمل الموزع بانتظام، وكذلك الحمل المركب من حمل موزع بانتظام وحمل مركز عند منتصف العارضة. وقد دلت النتائج على أن نوع الحمل المؤثر على العارضة له أثر كبير على انحرافها وذلك من خلال التأثير على مقدار عزم القصور الذاتي الفعّال للعارضة. وبناءً على نتائج البحث اقترح نموذج عام لحساب عزم القصور الذاتي الفعّال للعوارض الخرسانية تحت تأثير أي نوع من الأحمال المتماثلة. كما تم التحقق من دقة النموذج المقترح بالمقارنة مع النتائج المتوفرة لأبحاث سابقة.

---

* طالب دراسات عليا.